ADVANCES IN ATMOSPHERIC SCIENCES, VOL. 26, NO. 4, 2009, 748–762

Climate Responses to Direct Radiative Forcing of Anthropogenic Aerosols, Tropospheric Ozone, and Long-Lived Greenhouse Gases in Eastern China over 1951–2000

CHANG Wenyuan*[1,2,3] (常文渊), LIAO Hong[1] (廖 宏), and WANG Huijun[2,4] (王会军)

[1] *State Key Laboratory of Atmospheric Boundary Layer Physics and Atmospheric Chemistry, Institute of Atmospheric Physics, Chinese Academy of Sciences, Beijing* 100029

[2] *Nansen-Zhu International Research Center, Institute of Atmospheric Physics, Chinese Academy of Sciences, Beijing* 100029

[3] *Graduate University of Chinese Academy of Sciences, Beijing* 100049

[4] *Climate Change Research Center (CCRC), Chinese Academy of Sciences, Beijing* 100029

(Received 3 February 2009; revised 17 March 2009)

ABSTRACT

A unified chemistry-aerosol-climate model is applied in this work to compare climate responses to changing concentrations of long-lived greenhouse gases (GHGs, CO_2, CH_4, N_2O), tropospheric O_3, and aerosols during the years 1951–2000. Concentrations of sulfate, nitrate, primary organic carbon (POA), secondary organic carbon (SOA), black carbon (BC) aerosols, and tropospheric O_3 for the years 1950 and 2000 are obtained *a priori* by coupled chemistry-aerosol-GCM simulations, and then monthly concentrations are interpolated linearly between 1951 and 2000. The annual concentrations of GHGs are taken from the IPCC Third Assessment Report. BC aerosol is internally mixed with other aerosols. Model results indicate that the simulated climate change over 1951–2000 is sensitive to anthropogenic changes in atmospheric components. The predicted year 2000 global mean surface air temperature can differ by 0.8°C with different forcings. Relative to the climate simulation without changes in GHGs, O_3, and aerosols, anthropogenic forcings of SO_4^{2-}, BC, BC+SO_4^{2-}, BC+SO_4^{2-}+POA, BC+SO_4^{2-}+POA+SOA+NO_3^-, O_3, and GHGs are predicted to change the surface air temperature averaged over 1971–2000 in eastern China, respectively, by −0.40°C, +0.62°C, +0.18°C, +0.15°C, −0.78°C, +0.43°C, and +0.85°C, and to change the precipitation, respectively, by −0.21, +0.07, −0.03, +0.02, −0.24, −0.08, and +0.10 mm d^{-1}. The authors conclude that all major aerosols are as important as GHGs in influencing climate change in eastern China, and tropospheric O_3 also needs to be included in studies of regional climate change in China.

Key words: direct effect of aerosol, tropospheric ozone, greenhouse gases, transient simulation

Citation: Chang, W. Y., H. Liao, and H. J. Wang, 2009: Climate responses to direct radiative forcing of anthropogenic aerosols, tropospheric ozone, and long-lived greenhouse gases in eastern China over 1951–2000. *Adv. Atmos. Sci.*, **26**(4), 748–762, doi: 10.1007/s00376-009-9032-4.

1. Introduction

The long-lived greenhouse gases (CO_2, CH_4, and N_2O), tropospheric O_3, and aerosols have made significant contributions to global radiative forcing of the climate since preindustrial times (IPCC, 2007). GHGs and tropospheric O_3 lead to global warming, and aerosols influence the climate through absorption and scattering of radiation (the so-called direct effect) and through their influence on cloud properties (the so-called indirect effect).

There have been numerous assessments of climate change driven by GHGs (e.g., Keen and Murphy, 1997; Trenberth, 1999; Hansen et al., 2005; Levy et al., 2008; Shindell et al., 2008), tropospheric ozone (e.g., Ramaswamy and Bowen, 1994; Hansen et al., 1997; Stu-

*Corresponding author: CHANG Wenyuan, changwy@mail.iap.ac.cn

ber et al., 2001; Mickley et al., 2004; Shindell et al., 2006; Chen et al., 2007), and aerosols (Hansen et al., 1997; Boer et al., 2000; Menon et al., 2002; Jacobson, 2004; Wang, 2004; Chung and Seinfeld, 2005; Hansen et al., 2005; Ramanathan et al., 2005; Takemura et al., 2005; Stier et al., 2006; Roeckner et al., 2006; Wang, 2007; Chen et al., 2007; Shindell et al., 2008). Because of the coexistence of GHGs, tropospheric O_3, and multiple aerosol species in the atmosphere, all anthropogenic changes in the atmospheric components need to be considered in order to accurately simulate climate change. Most of the previous climate simulations only accounted for a fraction of anthropogenic changes in GHGs, tropospheric O_3, and aerosols. Several recent studies have compared the roles of forcings by different atmospheric species in climate change on a global scale (Hansen et al., 2005; Chen et al., 2007; Shindell et al., 2008; Levy et al., 2008), but none of these studies have focused on regional climate change in eastern China over the past decades.

China has been undergoing rapid industrial and economic development over the past two decades with increasing emissions of aerosols and gaseous pollutants. The concentrations of NO_2, one of the most important precursors of O_3, have been shown to increase largely over the past decade and are now among the highest values based on satellite retrieval (Zhang et al., 2007). Surface ozone data from the Linan Regional Background Station in eastern China showed that the monthly highest 5% ozone concentrations have been increasing over 1991–2006 (Xu et al., 2008). The measured $PM_{2.5}$ concentrations are within 72.6–129.9 μg m^{-3} in the winter and 49.1–107.5 μg m^{-3} in the summer in southern China (Cao et al., 2003, 2004; Duan et al., 2007); and about 78.0–208.4 μg m^{-3} in the winter and 80.3–121.7 μg m^{-3} in the summer in northern China (Dan et al., 2004; Yang et al., 2005; Yu et al., 2006). High concentrations of O_3 and aerosols suggest that it may be essential to consider both of them in the climate simulations for China.

We utilize in this work a unified tropospheric chemistry-aerosol model within the Goddard Institute for Space Studies general circulation model II' (GISS GCM II') (Liao et al., 2003, 2004; Liao and Seinfeld, 2005; Liao et al., 2006) to compare climate responses to forcings by GHGs, tropospheric O_3, and different combinations of aerosol species over 1951–2000, with a focus on the magnitude of changes in meteorological parameters in eastern China. Section 2 describes the model and experimental design. Section 3 presents simulated concentrations of tropospheric O_3 and aerosols for the years 1950 and 2000 as well as transient climate change simulated in the designed climate simulations. Climate responses including the changes in surface air temperature, precipitation, and surface energy balance will be discussed.

2. Model description and experimental design

2.1 *The unified model*

The unified tropospheric chemistry-aerosol model within the GISS GCM II' is described in detail in previous studies (Liao et al., 2003, 2004; Liao and Seinfeld, 2005; Liao et al., 2006). The GISS GCM II' has a horizontal resolution of 4° (lat) by 5° (lon), with 9 σ vertical layers from the surface to 10 hPa (Rind and Lerner, 1996; Rind et al., 1999) and is coupled with a "Q-flux" ocean (Hansen et al., 1984). In the Q-flux ocean, the monthly horizontal heat transport fluxes are held constant as in Mickley et al. (2004), while changes in the sea surface temperatures and sea ice are calculated based on the energy exchange with the atmosphere, ocean heat transport, and the ocean mixed layer heat capacity (Hansen et al., 1984; Russell et al., 1984). The GISS model has been used extensively to probe the climate's response to perturbations in GHG concentrations, solar luminosity, and tropospheric O_3 and aerosol burdens (e.g., Grenfell et al., 2001; Rind et al., 2001; Shindell et al., 2001; Menon, 2004; Mickley et al., 2004; Chung and Seinfeld, 2005; Chen et al., 2007).

The model includes a detailed simulation of tropospheric O_3-NO_x-hydrocarbon chemistry, as well as sulfate, nitrate, ammonium, BC, POA, SOA, sea salt, and mineral dust aerosols. The chemical mechanism includes 225 chemical species and 346 reactions for simulating gas-phase species and aerosols. The partitioning of ammonia and nitrate between the gas and aerosol phases is determined by the on-line thermodynamic equilibrium model ISORROPIA (Nenes et al., 1998), and the formation of secondary organic aerosols from monoterpenes is based on equilibrium partitioning and experimentally determined yield parameters (Griffin et al., 1999a,b; Chung and Seinfeld, 2002). Two-way coupling between the aerosols and gas-phase chemistry provides consistent chemical fields for the aerosol dynamics and the aerosol mass for heterogeneous processes and calculations of gas-phase photolysis rates.

The radiative effects of GHGs, O_3, and aerosols are fed back into the GISS GCM in climate simulations. BC aerosols are assumed to be internally mixed with other aerosol species in the simulations with mixed aerosols. The refractive index of the internally mixed aerosols is calculated by the volume-weighting of the refractive index of each aerosol species and associated water (Sloane, 1984, 1986; Sloane and Wolff, 1985; Sloane et al., 1991).

$$n = \frac{V_i n_i}{V}\ ,\ \ k = \frac{V_i k_i}{V}\ ,\ \ V = \sum_i V_i\ , \qquad (1)$$

where V_i is the volume of the species i including ammonium sulfate, nitrate, organic carbon, black carbon, and the water content of the aerosols. n_i and k_i are the real and imaginary parts of the refractive index of species i, respectively. The refractive index for each aerosol species follows that listed in Liao et al. (2004). The aerosol optical properties (extinction cross section, single-scattering albedo, and asymmetry factor) are calculated by the Mie theory based on wavelength-dependent refractive indices and aerosol size distributions. Assumptions and parameters used for the calculations of aerosol optical properties are given in Liao et al. (2004). Water uptake by sulfate/nitrate/ammonium aerosols is determined by the aerosol thermodynamic equilibrium module, ISORROPIA (Nenes et al., 1998). Water uptake by organic carbon aerosols follows the treatment of Chung and Seinfeld (2002). We only consider the aerosols' direct radiative effect in this work.

2.2 *Simulations of concentrations of O_3 and aerosols in years 1950 and 2000*

Concentrations of sulfate, nitrate, primary organic carbon, secondary organic carbon, black carbon, and tropospheric O_3 in the years 1950 and 2000 are obtained *a priori* by two fully coupled chemistry-aerosol-climate simulations, each integrating the unified model for 4 years. Present-day global anthropogenic emissions follow those listed in detail in Liao et al. (2006), except that anthropogenic emissions in Asia have been updated to use David Streets 2006 emissions inventories (http://www.cgrer.uiowa.edu/EMISSION_DATA_new/index_16.html). Natural emissions, including lightning NO_x, NO_x from soil, biogenic hydrocarbons, and dimethyl sulfide (DMS), are estimated based on simulated meteorological conditions (Liao et al., 2006). In the year 1950, all anthropogenic emissions in the model are set to zero. Monthly concentrations averaged over the final two months of the year 1950 (or year 2000) simulation are used to represent the concentrations and distributions of ozone and aerosols for year 1950 (or year 2000). These concentrations are then interpolated linearly between 1950 and 2000 for the transient climate simulations over 1951–2000.

2.3 *Transient climate simulations*

Table 1 lists all experiments performed to examine the climate responses to forcings by GHGs, tropospheric O_3, and different combinations of aerosol species over 1951–2000. The control run, denoted as CTRL1950, is the climate simulation with concentrations of GHGs, tropospheric O_3, and aerosols fixed at year 1950 levels. Simulation ΔGHG is performed with interpolated annual changes in concentrations of GHGs over the years 1951–2000, but concentrations of tropospheric O_3 and aerosols are fixed at year 1950 levels. Additional experiments are designed as ΔGHG+ΔXX, where ΔXX represents one of the cases of ΔBC, ΔSO4, ΔBCSO4, ΔBCSO4POA, ΔAER, and ΔAERO3, with, respectively, changing concentrations of BC, SO_4^{2-}, BC+SO_4^{2-}, BC+SO_4^{2-}+POA, BC+SO_4^{2-}+POA+NO_3^-+SOA, and BC+SO_4^{2-}+POA+NO_3^-+SOA+O_3 over 1951–2000. The difference between simulations ΔGHG and CTRL1950 represents climate change over 1951–2000 driven by anthropogenic changes in GHGs, while the difference between simulations ΔGHG+ΔXX and ΔGHG assesses climate change over 1951–2000 driven by anthropogenic changes in aerosol (or a combination of aerosols) XX.

All the simulations in Table 1 are initialized us-

Table 1. Summary of transient climate simulations.

	Experiment	Period of long-lived greenhouse gases	Period of aerosols	Period of tropospheric ozone
1	CTRL1950	1950	1950	1950
2	ΔGHG	1951–2000	1950	1950
3*	ΔGHG+ΔBC	1951–2000	BC changes over 1951–2000	1950
	ΔGHG+ΔSO4		SO_4^{2-} changes over 1951–2000	1950
	ΔGHG+ΔBCSO4		BC and SO_4^{2-} change over 1951–2000	1950
	ΔGHG+ΔBCSO4POA		BC, SO_4^{2-}, and POA change over 1951–2000	1950
	ΔGHG+ΔAER		BC, SO_4^{2-}, POA, NO_3^-, and SOA change over 1951–2000	1950
	ΔGHG+ΔAERO3		BC, SO_4^{2-}, POA, NO_3^-, and SOA change over 1951–2000	1951–2000

*Concentrations of aerosol species that are not allowed to change over 1951–2000 are kept at 1950 levels.

Table 2. Predicted annual mean global burdens (Tg) of aerosols and ozone.

	SO_4^{2-}	NO_3^-	BC	POA	SOA	O_3
1950	0.63	0.30	0.007	0.07	0.26	229.36
2000	2.30	0.52	0.14	0.79	0.33	364.11
2000–1950	1.67	0.22	0.13	0.72	0.07	134.75

Table 3. Predicted mean tropopause anthropogenic radiative forcing (W m^{-2}) by the changes in greenhouse gases, tropospheric ozone, and aerosols (SO_4^{2-}, NO_3^-, POA, SOA, and BC) over 1950–2000.

	Region	DJF	JJA	Annual mean
GHG	Global	1.93	1.94	1.94
	Eastern China	1.86	1.73	1.79
O_3	Global	0.41	0.58	0.51
	Eastern China	0.57	1.16	0.87
Aerosol	Global	−0.58	−0.56	−0.57
	Eastern China	−5.39	−6.49	−6.08

ing meteorological fields archived at the end of a 30-year spin-up simulation with year 1950 concentrations of GHGs, tropospheric O_3, and aerosols. Each transient climate simulation is integrated from 1951 to 2000. Concentrations of GHGs over 1950–2000 are obtained by spline interpolation from those reported in the IPCC Third Assessment Report (IPCC, 2001); concentrations of CO_2, CH_4, and N_2O are, respectively, 320.18, 1.1063, and 0.2919 ppm in the year 1951, and 369.01, 1.7500, and 0.3152 ppm in the year 2000.

3. Model results

3.1 *Global concentrations of O_3 and aerosols in years 1950 and 2000*

Figure 1 shows the simulated annual mean column concentrations of aerosols and tropospheric O_3 in 1950 and 2000. As expected, concentrations in 1950 are generally small in the absence of anthropogenic emissions. Sulfate and SOA have relatively higher concentrations as compared to other aerosol species in 1950; sulfate formation is mostly from natural DMS emissions over the oceans, and SOA formation is from the biogenic emissions of hydrocarbons. In 2000, column burdens of all aerosol species and O_3 show high values over populated areas.

Predicted annual and global mean burdens of aerosols and O_3 in the years 1950 and 2000 are given in Table 2. Sulfate is the most abundant aerosol in the atmosphere in both time periods. The sulfate burden of 0.63 Tg is about twice the nitrate burden of 0.30 Tg or the SOA burden of 0.26 Tg in 1950. In the year 2000, the global burdens of sulfate and POA show large increases relative to those in 1950; sulfate and POA increase by 1.67 Tg and 0.72 Tg, respectively. The increase in the BC burden of 0.13 Tg over 1950–2000 is relatively small as compared with the changes in the burdens of sulfate and POA, but it can have a large impact on the climate because of its unique optical properties. The tropospheric O_3 burden in 2000 is 1.6 times the value in 1950.

3.2 *Anthropogenic radiative forcing by GHGs, O_3, and aerosols over 1950–2000*

We compute the direct radiative effect (DRE) of a species as the difference in the net flux with and without the species, and then calculate anthropogenic forcing as the change in DRE from 1950 to 2000. Figure 2 shows the horizontal distributions of anthropogenic radiative forcing at the tropopause in 2000 relative to 1950. Radiative forcing by GHGs is relatively uniform as compared to that of O_3 or other aerosols. Tropospheric O_3 forcing is significant in the Northern Hemisphere and larger in JJA (June–July–August) than in DJF (December–January–February), because of the strong photochemical reactions in JJA. The warming by O_3 over eastern China (20°–50°N, 100°–130°E) is 1.16 W m^{-2} in JJA (Table 3). Large cooling by all aerosol species (SO_4^{2-}, NO_3^-, POA, SOA, and BC) is predicted over the industrialized areas and over Central Africa and South America where biomass burning is significant. We also compare in Table 3 the forcings by GHGs, O_3, and aerosols in eastern China. The slightly stronger cooling exists in eastern China in JJA than in DJF despite of the lower anthropogenic emissions (Streets et al., 2003), stronger diffusion/convection, shifting of the aerosol thermodynamic equilibrium to a gas-phase at warmer temperatures (Dawson et al., 2007), and the larger wet deposition associated with the Asian summer monsoon[a].

[a]Zhang, L., H. Liao, and J. P. Li, 2009: Impacts of Asian Summer Monsoon on Seasonal and Interannual Variations of Aerosols over Eastern China, submitted to *J. Geophys. Res.*

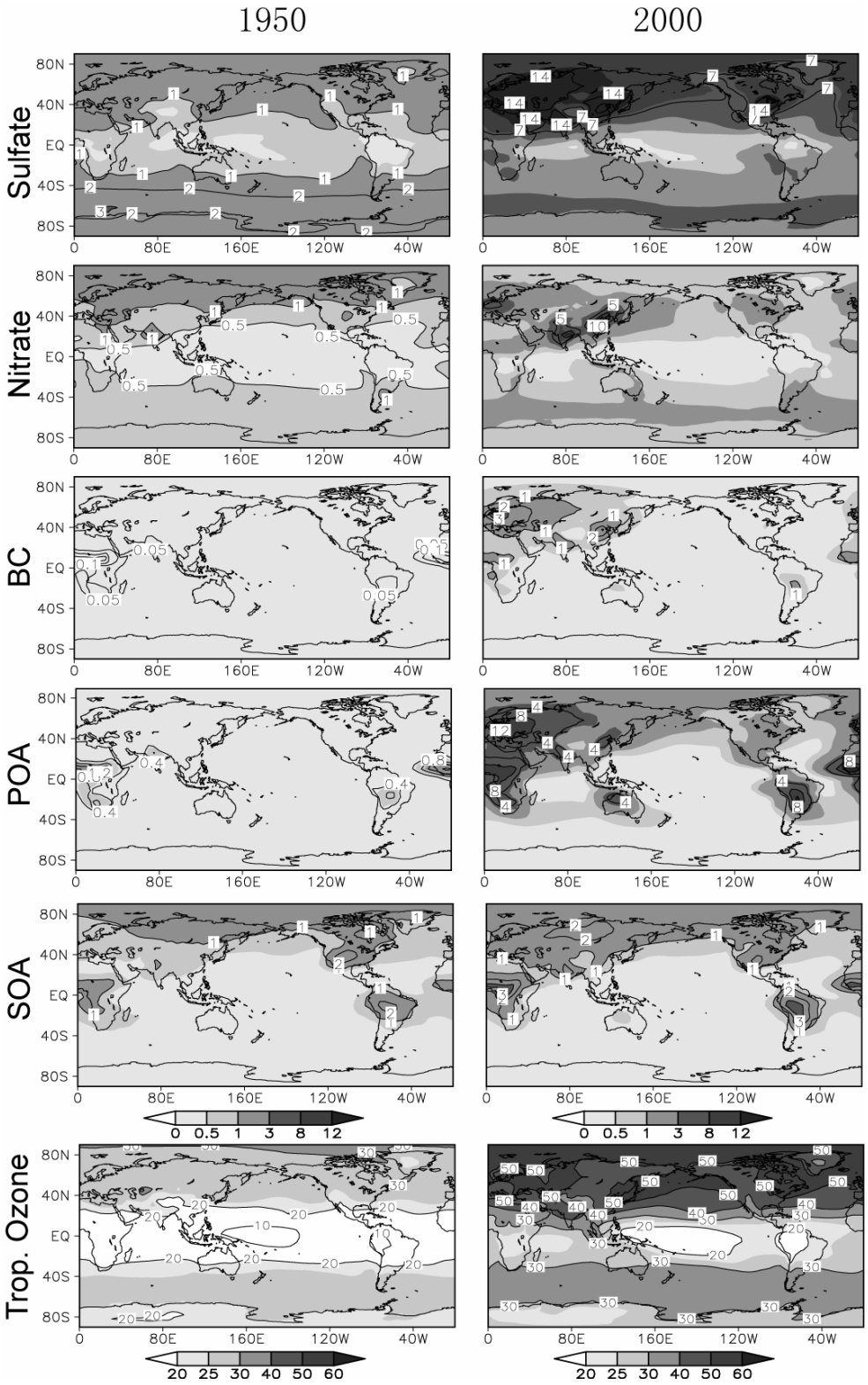

Fig. 1. Predicted annual mean column of burdens of the aerosols (mg m^{-2}) and tropospheric ozone (DU) in 1950 and 2000.

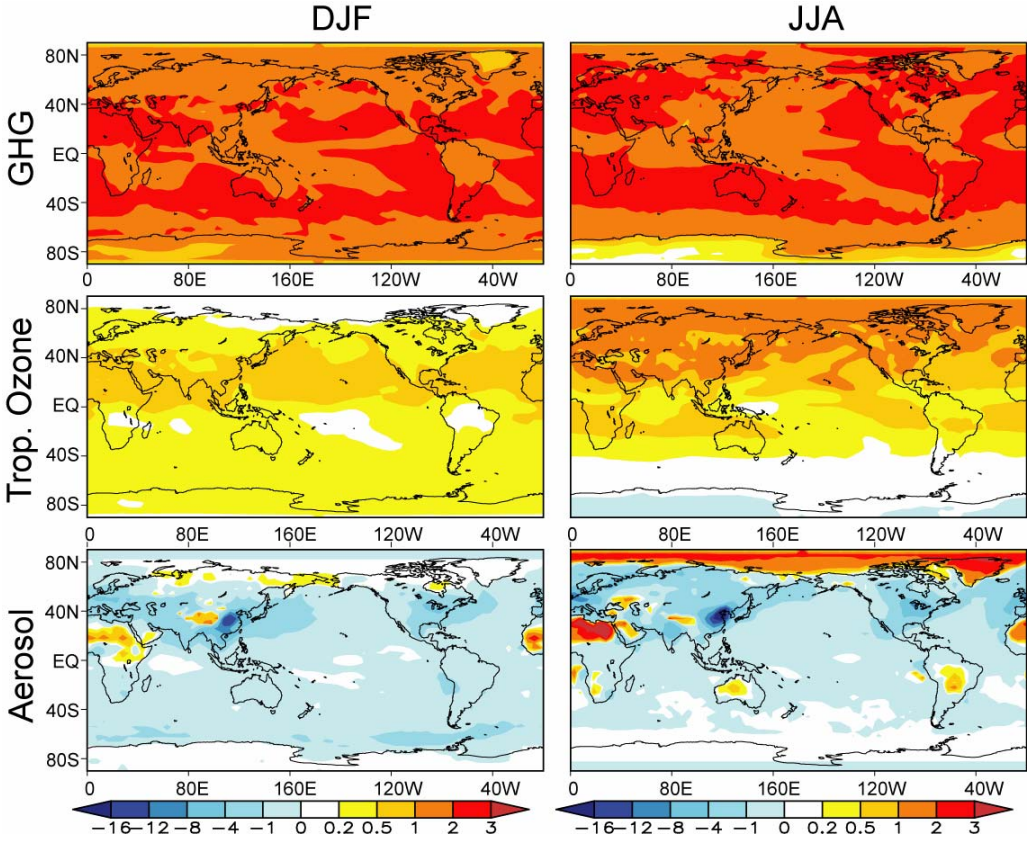

Fig. 2. Predicted seasonal mean tropopause anthropogenic radiative forcing (W m^{-2}) by greenhouse gases, tropospheric ozone, and all aerosols (SO_4^{2-}, NO_3^-, POA, SOA, and BC) from 1950 to 2000. Negative values indicate cooling. DJF represents December–January–February and JJA for June–July–August.

3.3 *Climate responses to direct radiative forcing of anthropogenic aerosols, tropospheric O_3, and GHGs*

3.3.1 *Responses in surface air temperature (SAT)*

Figure 3 shows predicted changes in the global annual mean SAT over 1951–2000 from all the simulations described in section 2.3. GHGs are the most important factors that lead to the increases in SAT; a warming trend is predicted in all simulations with increases in GHGs. Consideration of aerosols and O_3 in climate simulations does not change the general warming trend in the simulated global mean SAT, but does cause a 0.8°C difference in the simulated year 2000 global mean SAT between simulations ΔBC and ΔAER. The simulations ΔBC, ΔBCSO4, ΔBCSO4POA (note changes in GHGs are included in all the simulations except CTRL1950) predict a higher year 2000 SAT than the simulation ΔGHG, because of the absorption by BC and the assumed internal mixing of BC with scattering species. Relative to the year 2000 global mean SAT of 15.1°C simulated in ΔGHG,

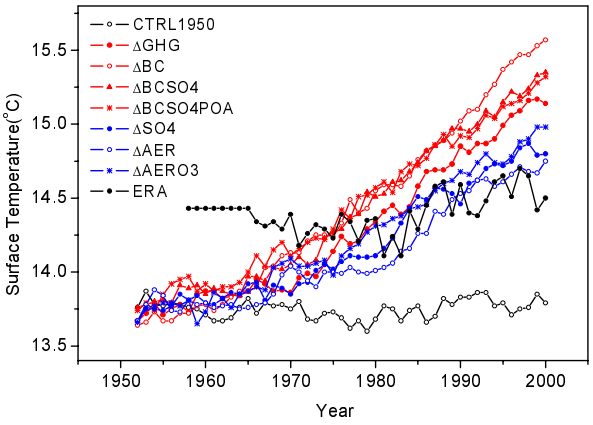

Fig. 3. Predicted changes in the global annual mean surface air temperature (°C) over 1951–2000 from all the simulations listed in Table 1.

BC aerosols lead to an additional warming of 0.5°C in ΔBC. In ΔBCSO4POA, the addition of the scattering aerosol of sulfate and POA cannot offset all of the warming by BC. Simulations ΔSO4 and ΔAER predict a lower year 2000 SAT than ΔGHG. When all

aerosol species are considered in ΔAER, the predicted global mean year 2000 SAT differs from that in ΔBC by 0.8°C, indicating the importance of the inclusion of all major aerosol species in climate simulations. The net effect of O_3 and all the aerosols is a cooling of the climate relative to simulation ΔGHG. The modeled global mean temperatures in ΔAERO3 during 1971–2000 are generally warmer than those in ΔAER. The global mean temperatures simulated in ΔAER are closer to the ERA40 reanalysis data than those simulated in ΔAERO3 after the 1990s, which might be caused by the uncertainty in simulating aerosol cooling.

Climate response to forcings by different atmospheric components can be further examined by comparing averaged meteorological parameters over 1971–2000 in the sensitivity studies with those from ΔGHG run for O_3 and aerosols (or the CTRL1950 for green house gases). The geographical distributions of SAT responses obtained from each of the sensitivity runs are shown in Fig. 4. There are two major features in the simulated SAT responses. The first is that the SAT responses are the largest in the high latitudes independent of the type of forcing (i.e., GHGs, O_3, or different aerosol species), because of the sea-ice climate feedbacks. For example, the surface cooling by aerosols can lead to an extension of sea-ice coverage in the high latitudes, increasing surface albedo and hence further reducing solar radiation and temperature at the surface. The reverse is true if there is a positive forcing (warming) in the high latitudes. Such sea-ice climate feedbacks agree with results in previous studies (Hansen et al., 1997; Forster et al., 2000; Boer and Yu, 2003; Joshi et al., 2003; Mickley et al., 2004; Chung and Seinfeld, 2005). As a result, the distribution of SAT responses does not necessarily follow that of the direct radiative forcing and the maximum response does not occur over regions with the largest forcing. The second feature is that, for short-lived species (O_3 and aerosols), responses in SAT are large over or in the downwind regions of populated areas where anthropogenic emissions are the highest.

It can be seen clearly from the case of ΔBCSO4 in Fig. 4 that the cooling induced by sulfate aerosols can only partly offset the warming by black carbon on a global mean basis. This result is different from the work of Jones et al. (2007) who found that the cooling by sulfate is larger than the warming by black carbon in equilibrium climate simulations. The difference arises because BC and sulfate are assumed to be mixed externally in Jones et al. (2007), whereas they are assumed to be an internal mixture in our study. An internal mixture has been shown to have stronger warming than an external mixture (Chung and Seinfeld, 2002). Over eastern China, the internal mixing of BC and sulfate leads to weak cooling in DJF and statistically significant warming in JJA.

The pattern of responses in SAT in simulation ΔBCSO4POA is similar to that obtained in ΔBCSO4, because POA is a weak absorbing species with a single-scattering albedo of 0.96 (Liao et al., 2004). The introduction of POA to the simulation reduces the statistical significance of the warming but cannot offset the warming. In simulation ΔAER, with all of BC, SO_4^{2-}, POA, SOA, and NO_3^- aerosols considered, a general global cooling is predicted; the average reduction in the global annual mean SAT is −0.26°C, which is 1.7 times of the cooling by sulfate alone (Fig. 4). The maximum cooling exceeding 1.5°C in DJF and 0.5°C−1.0°C in JJA are predicted in eastern China in ΔAER. Besides that, aerosol concentrations over eastern China are lower in JJA than in DJF as a result of the large wet deposition associated with the Asian summer monsoon, more stable lapse rates in DJF than in JJA confines the temperature responses closer to the surface in DJF.

Tropospheric O_3 and GHGs lead to general warming. While both GHGs and O_3 lead to strong warming over the high latitudes, tropospheric O_3 also largely increases the SAT over populated areas. The predicted change in the global and annual mean SAT by tropospheric O_3 is 0.16°C, which is slightly lower than the global annual mean warming of 0.22°C by BC and is about 21% of the 0.77°C global warming by GHGs.

It is of interest to compare the magnitude of changes in SAT over eastern China (Table 4). Only two of all the simulations predict a cooling over eastern China; ΔSO4 and ΔAER predict a cooling of

Table 4. Summary of the averaged changes of selected climate variables over 1971–2000 in eastern China (20°–50°N, 100°–130°E).

	ΔSO4	ΔBC	ΔBCSO4	ΔBCSO4POA	ΔAER	ΔO3	ΔGHG
Temperature (°C)	−0.40	0.62	0.18	0.15	−0.78	0.43	0.85
Radiation (W m^{-2})	−1.09	−0.91	−2.71	−2.98	−7.29	0.40	1.12
Latent heat (W m^{-2})	1.92	−0.55	1.38	1.17	5.18	−0.86	−2.26
Sensible heat (W m^{-2})	−1.03	1.41	1.37	1.83	1.67	0.73	1.34
Precipitation (mm d^{-1})	−0.21	0.07	−0.03	0.02	−0.24	0.08	0.10

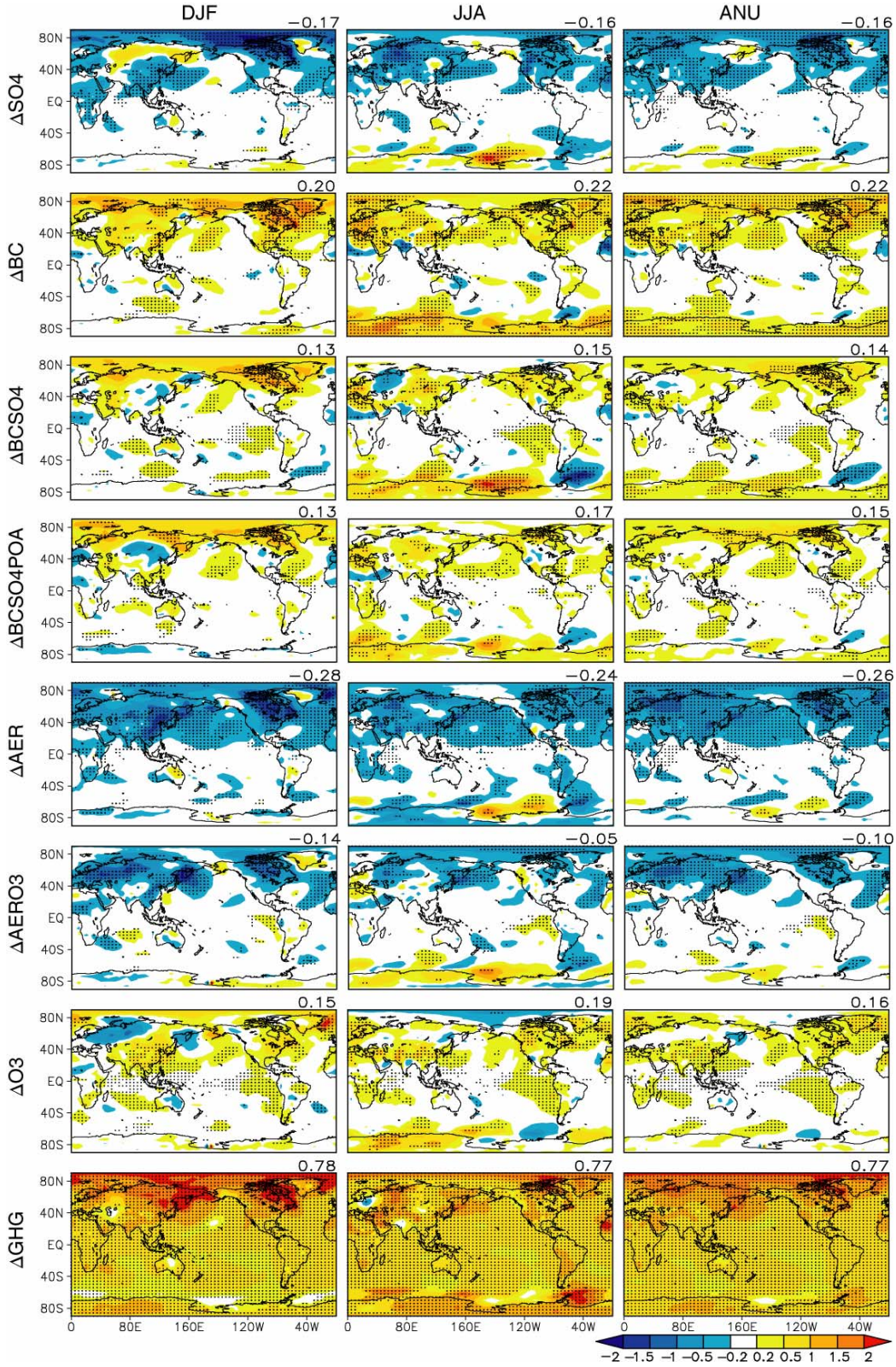

Fig. 4. Predicted differences in DJF, JJA, and the annual mean surface air temperature (°C) over 1971–2000 between each of the sensitivity studies and the ΔGHG simulation for top seven rows. The differences are between simulation ΔGHG and the CTRL1950 run for bottom row. Dotted areas denote results that pass the *t*-test at the 95% confidence level. The global mean value is indicated at the top right corner of each panel.

0.40°C and 0.78°C, respectively. The largest warming of 0.85°C is predicted in ΔGHGs, followed by warming of 0.62°C in ΔBC, 0.43°C in ΔO_3, 0.18°C in ΔBCSO4, and 0.15°C in ΔBCSO4POA. The aerosol direct cooling of −0.78°C is close in magnitude to the warming of 0.85°C by GHGs, and the warming by tropospheric O_3 is 0.43°C in eastern China. These results indicate that it is important to consider effects of tropospheric O_3 and all aerosols in simulations of climate change in China.

3.3.2 *Responses in precipitation*

The predicted responses of precipitation to changes in concentrations of different atmospheric components are shown in Fig. 5. Aerosol cooling usually reduces SAT, convection, evaporation, and hence precipitable water in the air, leading to reduced precipitation (Mitchell and Johns, 1997). On the contrary, a warming at the surface usually increases convection and evaporation, increasing regional precipitation. Such changes in precipitation can easily be identified in DJF when climate responses are quite confined to the surface. The presence of scattering aerosols is predicted to reduce precipitation in DJF over eastern China in all the cases of ΔSO4, ΔBCSO4, ΔBCSO4POA, ΔAER, and ΔAERO3 (Fig. 5). In JJA, the presence of sulfate aerosols in ΔSO4 is predicted to reduce precipitation in eastern China, and BC generally increases precipitation in eastern China except the Yangtze River basin.

On a global mean basis, simulations with all anthropogenic aerosol species (ΔAER and ΔAERO3) show statistically significant reductions in precipitation over heavily polluted areas such as eastern China and Europe. GHGs are predicted to generally increase precipitation over the mid-high latitudes, which is consistent with the multi-model predictions in IPCC (2007).

In eastern China, the annual mean changes in precipitation of −0.21 and +0.07 mm d^{-1} are predicted in ΔSO4 and ΔBC, respectively (Table 4). The reduction in precipitation in eastern China in ΔAER is about the same as that simulated in ΔSO4, and the reduction is larger than the increase in precipitation in ΔGHG (Table 4), indicating that in China, aerosols have larger impacts on the hydrological cycle than GHGs. Note that the indirect effect of aerosols is not considered in this work, which is expected to have additional large impacts on the regional precipitation in China.

It should be noted that in simulations of both ΔBC and ΔAER, the simulated pattern of changes in precipitation in JJA does not agree with the observed pattern of "southern flood and northern drought". Although Menon et al. (2002) reproduced the observed changes in JJA precipitation in China by considering the absorption of BC aerosols in their climate simulation, their simulation was based on fixed SST and an assumption of a uniform aerosol single scattering albedo of 0.85. The responses of the oceans to external forcing are very important to summer precipitation in southern China, since the regional moisture convergence depends on the large-scale circulation related to SST. Menon et al. (2002) (same study) also found that there could be less precipitation once observed changes of SST were used in the climate simulation. Meehl et al. (2008) studied the climatic effect of BC on the Indian and Asian summer monsoon with dynamic oceans and reported a reduced summer precipitation in southern China as well. However, we cannot conclude that the changes in precipitation in China are not caused by aerosols, because the indirect effect of aerosols is not considered in this work. Recent work by Rosenfeld et al. (2008) has shown that the indirect effect of aerosols can increase the precipitation of deep convective clouds, which might be very important for southern China with strong deep convection associated with the Asian summer monsoon.

3.3.3 *Changes in the surface energy budget*

(1) Global changes in radiative flux

Responses in SAT and precipitation are associated with the changes in the energy balance induced by changing atmospheric components. Figure 6a shows the differences in the surface-layer net radiative flux (shortwave radiation plus longwave radiation) averaged over 1971–2000 between each sensitivity study and the ΔGHG simulation for O_3 and aerosols (or the CTRL1950 for green house gases). Negative values represent reductions in the net radiation that reaches the Earth's surface. Sulfate aerosols scatter solar radiation back to outer space, reducing the shortwave radiation that reaches the surface. Black carbon aerosols reduce solar radiation by both scattering and absorbing solar radiation. With all the feedbacks in the atmosphere and the surface (for example, changes in evaporation, ice cover, and snow cover), all simulations with aerosols show reductions in the annual and global mean surface-layer net radiation; a reduction of 0.40 W m^{-2} is predicted in the presence of sulfate aerosols in ΔSO4, and that of 0.11 W m^{-2} is predicted in ΔBC. For cases with mixed aerosols, the annual and global mean reductions are larger with more aerosol species added in a climate simulation; the reductions in the global and annual mean surface-layer net radiation in ΔBCSO4, ΔBCSO4POA, ΔAER are, respectively, −0.46, −0.60, and −1.35 W m^{-2} (Fig. 6a). Although the atmosphere is absorbing solar radiation in the presence of BC in these simulations, the reduc-

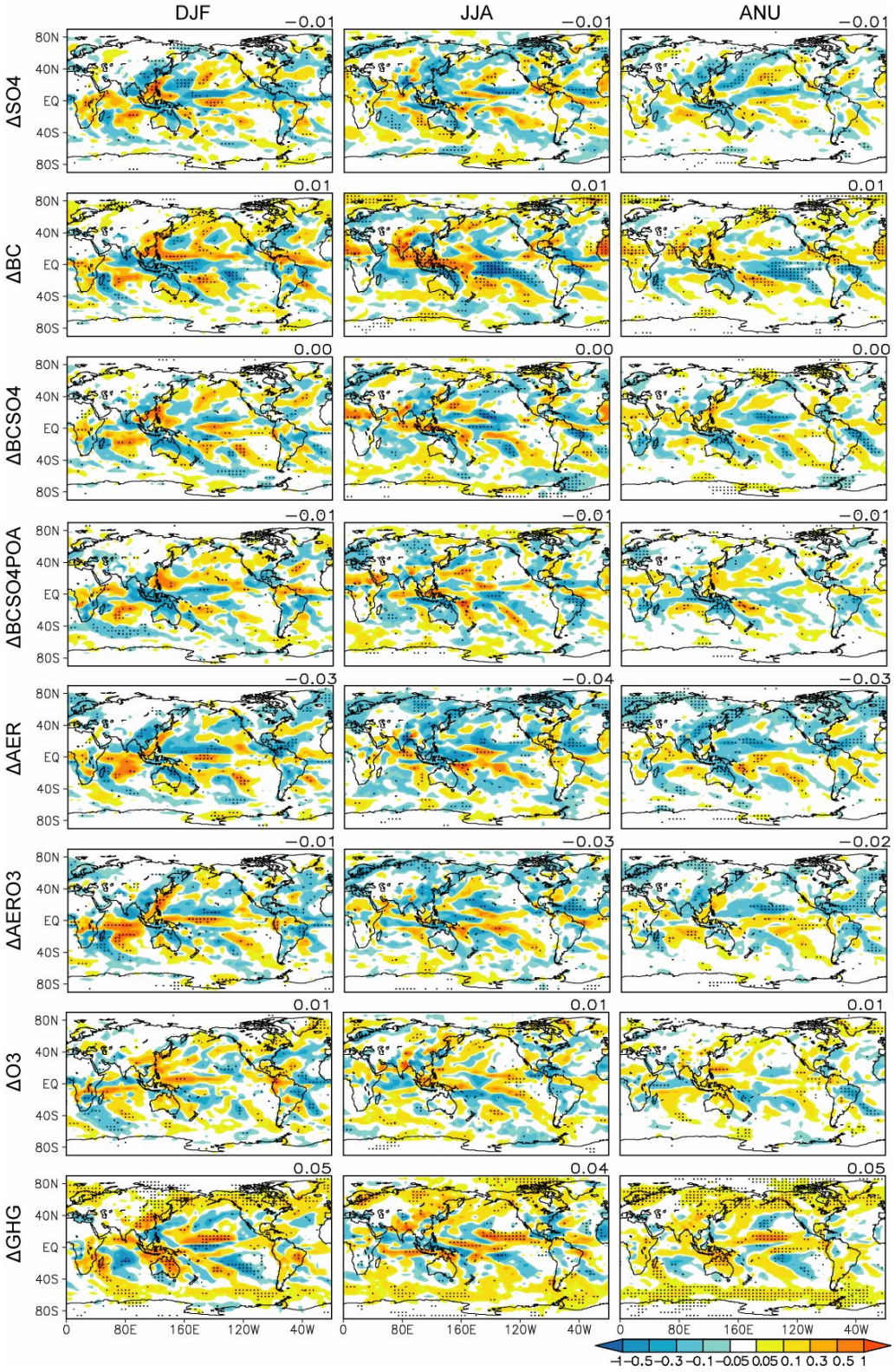

Fig. 5. Predicted differences in DJF, JJA, and the annual mean precipitation (mm d^{-1}) over 1971–2000 between each of the sensitivity studies and the ΔGHG simulation for top seven rows. The differences are between simulation ΔGHG and the CTRL1950 run for bottom row. Dotted areas denote results that pass the *t*-test at the 95% confidence level. The global mean value is indicated at the top right corner of each panel.

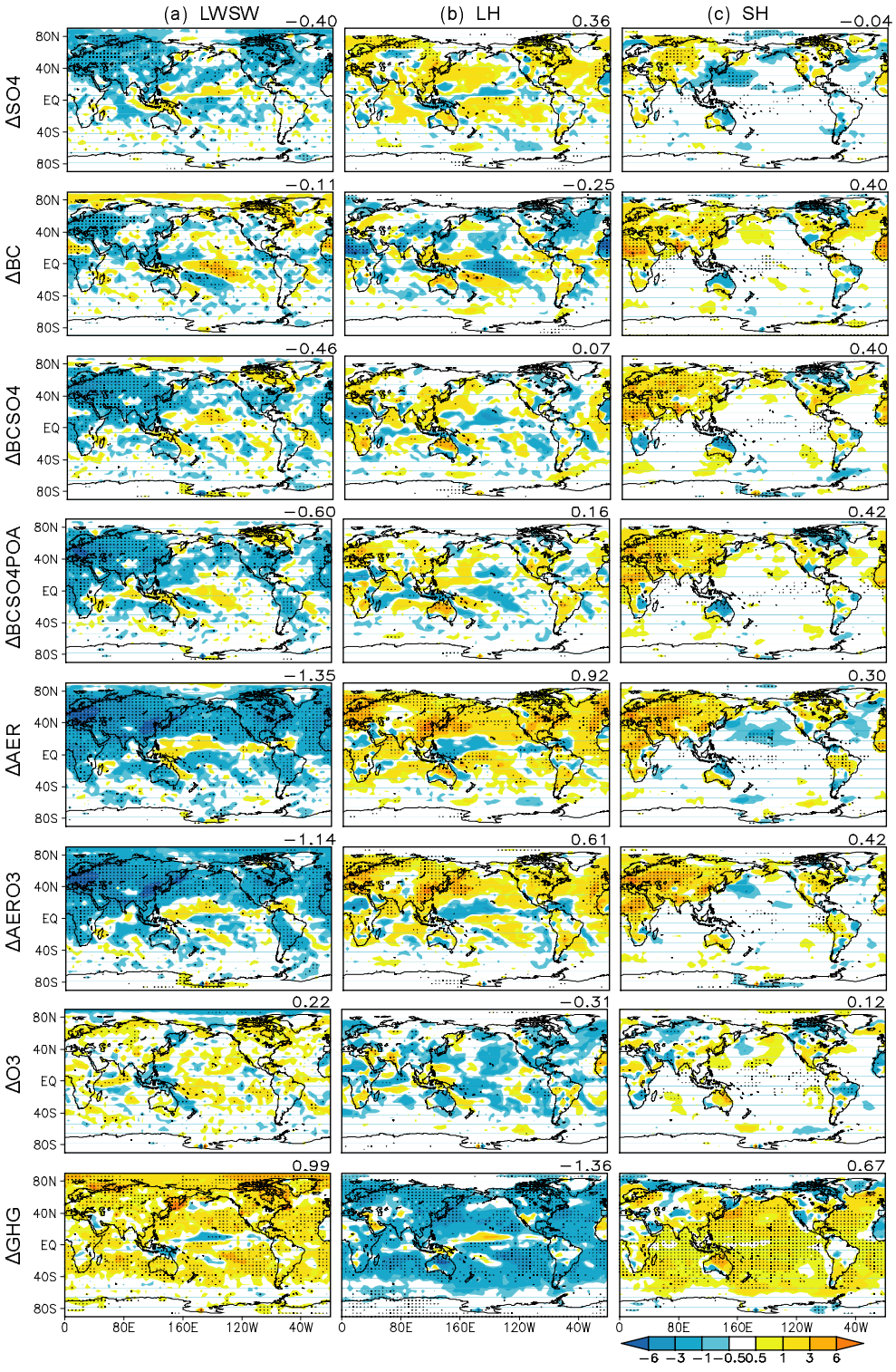

Fig. 6. Predicted differences in the energy flux (W m^{-2}) averaged over 1971–2000 between each of the sensitivity studies and the ΔGHG simulation for top seven rows. The differences are between simulation ΔGHG and the CTRL1950 run for bottom row. (a) Net radiative flux (shortwave plus longwave, LWSW). Negative values indicate reductions in the radiative flux that reach the surface. (b) Latent heat flux (LH). Positive values denote an increase in latent heat as a result of the reduced evaporation. (c) Sensible heat flux (SH). Positive values represent the downward transport of sensible heat. Dotted areas denote results that pass the *t*-test at the 95% confidence level. The global mean value is indicated at the top right corner of each panel.

tions in the net radiation indicate that the downward longwave radiation by warmed air cannot compensate the loss of solar radiation by aerosols, as shown by Liepert et al. (2004) and Wild et al. (2004). On an annual and global mean basis, tropospheric O_3 and GHGs increase the net radiative flux at the surface by 0.22 and 0.99 W m^{-2}, respectively, which are lower than the reduction of 1.35 W m^{-2} by all aerosol species in ΔAER.

(2) Global changes in latent heat flux

The changes in the net radiative fluxes reaching the surface and the consequent changes in SAT (Fig. 3) lead to changes in evaporation. Figure 6b shows the differences in the surface-layer latent heat flux averaged over 1971–2000 between each sensitivity study and the ΔGHG simulation for O_3 and aerosols (or the CTRL1950 for green house gases). Positive values represent increases of energy at the surface as a result of the reduced evaporation. The predicted annual and global mean latent heat flux increases in all cases with scattering aerosols. Species with a positive forcing (BC, tropospheric O_3, and GHGs) lead to increases in SAT (Fig. 3) and hence increased evaporation and reduced latent heat at the surface. In simulations ΔBCSO4 and ΔBCSO4POA, the global mean changes in latent heat flux are +0.07 and +0.16 W m^{-2}, respectively, which are smaller in magnitude than the +0.36 W m^{-2} in ΔSO4 and −0.25 W m^{-2} in ΔBC. With all major aerosol species in simulation ΔAER, the geographical distribution of the changes in the latent heat flux mimics that of the changes in the net radiative flux, although the changes in these two fluxes have opposite signs. The reductions in the annual and global mean latent flux by tropospheric O_3 and GHGs are −0.31 and −1.36 W m^{-2}, respectively. Results indicate that the changes in the energy balance are very sensitive to the atmospheric components considered in the simulations.

(3) Global changes in sensible heat flux

Sensible heat fluxes (Fig. 6c) are determined by differences in temperature between the atmosphere and the surface. Positive values represent energy moving from the atmosphere to the surface. The scattering and absorbing aerosols have different impacts on the sensible heat flux. Sulfate aerosols lead to a stronger reduction in SAT than in ground temperatures over eastern China and the North Pole, leading to a small negative global mean change in the sensible heat flux of −0.04 W m^{-2}. In the presence of mixed aerosols (scattering aerosols plus BC), the absorption by aerosols increases the atmospheric temperature, leading to the transport of sensible heat from the atmosphere to the surface; the global and annual mean sensible heat fluxes are within the range of 0.30–0.42 W m^{-2} in these cases. Over areas with a high surface albedo, such as the Sahara desert and central Asia, BC or mixed aerosols can absorb both incoming and reflected solar radiation, leading to large heating in the atmosphere and large downward sensible fluxes (Fig. 6c). Both tropospheric O_3 and GHGs lead to downward fluxes of the sensible heat. The global and annual mean downward transport of sensible heat is 0.12 W m^{-2} by tropospheric O_3 and 0.67 W m^{-2} by GHGs.

(4) Changes in the energy balance over eastern China

Table 4 shows the annual mean changes in energy fluxes in the presence of different atmospheric components in eastern China. The reduction in the net radiative flux at the surface in ΔAER is −7.29 W m^{-2}, which is about 2–7 times the reductions in other simulations with aerosols and about 5 times the total increase in the net radiative flux by tropospheric O_3 and GHGs. The positive change of latent heat of 5.18 W m^{-2} in ΔAER is about 5–10 times higher in magnitude than either the positive or negative changes in aerosol simulations, and it is about 2 times the reductions by O_3 and GHGs. Although a prevalent cooling is simulated in both the ΔSO4 and ΔAER experiments, the inclusion of black carbon in ΔAER leads to a downward flux of sensible heat of 1.67 W m^{-2}, which is opposite to the upward flux of 1.03 W m^{-2} in ΔSO4. The magnitude of the change in the sensible heat in ΔAER is larger than that in ΔGHG. Because of the high concentrations of tropospheric O_3, changes in the energy balance by O_3 are of the same sign as those by GHGs, with the magnitude of the changes about 30%–50% of the corresponding changes in ΔGHG. These results indicate that it is important to consider all major aerosol species in the examination of the energy balance at the surface in eastern China.

4. Summary

Climate responses to changes in concentrations of aerosols, tropospheric O_3, and long-lived greenhouse gases over 1951–2000 are compared based on a number of transient climate simulations using the GISS GCM II'. We considered 5 combinations of aerosols, including cases of ΔSO4, ΔBC, ΔBCSO4, ΔBCSO4POA, and ΔAER. The first four cases include aerosol species that are commonly considered in previous climate simulations, while ΔAER has additional aerosol species of nitrate and SOA.

On a global mean basis, the long-lived greenhouse gases are predicted to dominate the increases in the surface air temperature during the past decades. Such

a major role of GHGs in influencing the global mean surface air temperature was also reported in Levy et al. (2008) and Shindell et al. (2008). Aerosols and tropospheric O_3 are also found to be very important; with the same changes in concentrations of GHGs in all simulations, the predicted year 2000 global mean surface air temperature can differ by 0.8°C with additional forcings by tropospheric ozone and aerosols when different combinations of aerosols are assumed.

As a result of the high concentrations of O_3 and aerosols in eastern China, O_3 and aerosols play more significant roles in regional climate change in China than in globally averaged climate change. Averaged over eastern China, the responses in surface air temperature are +0.85°C, +0.43°C, and −0.78°C, respectively, to forcings of GHGs, tropospheric O_3, and all major aerosol species. In eastern China, all aerosols have an effect of reducing precipitation by −0.24 mm d^{-1}, while tropospheric O_3 and GHGs increase precipitation by 0.08 and 0.10 mm d^{-1}, respectively. Results suggest that besides the commonly considered aerosol species of sulfate, BC, and POA, nitrate and SOA should also be considered in studies of climate change.

There are some uncertainties associated with our model results. First, the mixed-layer ocean may prevent the heat fluxes from being transported into the deep ocean. Second, in this work we interpolated the concentrations of O_3 and aerosols between 1950–2000; more accurate simulations need to account for the historical changes in anthropogenic emissions. Final, the indirect effect of aerosols needs to be taken into account. All these issues will be improved in our subsequent studies.

Acknowledgements. This work is supported by the National Natural Science Foundation of China (Grant Nos. 90711004 and 40825016) and by the Chinese Academy of Sciences (Grant Nos: KZCX2-YW-Q1-02, KZCX2-YW-Q11-03).

REFERENCES

Boer, G. J., G. Flato, M. C. Reader, and D. Ramsden, 2000: A transient climate change simulation with greenhouse gas and aerosol forcing: Experimental design and comparison with the instrumental record for the twentieth century. *Climate Dyn.*, **16**, 405–425.

Boer, G. J., and B. Yu, 2003: Climate sensitivity and response. *Climate Dyn.*, **20**, 415–429.

Cao, J. J., S. C. Lee, K. F. Ho, X. Y. Zhang, S. C. Zou, K. Fung, J. C. Chow, and J. G. Watson, 2003: Characteristics of carbonaceous aerosol in Pearl River Delta Region, China during 2001 winter period. *Atmos. Environ.*, **37**, 1451–1460.

Cao, J. J., S. C. Lee, K. F. Ho, S. C. Zou, K. Fung, Y. Li, J. G. Watson, and J. C. Chow, 2004: Spatial and seasonal variations of atmospheric organic carbon and elemental carbon in Pearl River Delta Region, China. *Atmos. Environ.*, **38**, 4447–4456.

Chen, W.-T., H. Liao, and J. H. Seinfeld, 2007: Future climate impacts of direct radiative forcing of anthropogenic aerosols, tropospheric ozone, and long-lived greenhouse gases. *J. Geophys. Res.*, **112**, D14209, doi: 10.1029/2006JD008051.

Chung, S. H., and J. H. Seinfeld, 2002: Global distribution and climate forcing of carbonaceous aerosols. *J. Geophys. Res.*, **104**, doi: 10.1029/2001JD 001397.

Chung, S. H., and J. H. Seinfeld, 2005: Climate response of direct radiative forcing of anthropogenic black carbon. *J. Geophys. Res.*, **110**, doi: 10.1029/2004JD005441.

Dan, M., G. Zhuang, X. Li, H. Tao, and Y. Zhuang, 2004: The characteristics of carbonaceous species and their sources in $PM_{2.5}$ in Beijing. *Atmos. Environ.*, **38**, 3443–3452.

Dawson, J. P., P. J. Adams, and S. N. Pandis, 2007: Sensitivity of $PM_{2.5}$ to climate in the eastern US: a modeling case study. *Atmospheric Chemistry and Physics*, **7**, 4295–4309.

Duan, J., J. Tan, D. Cheng, X. Bi, W. Deng, G. Sheng, J. Fu, and M. H. Wong, 2007: Sources and characteristics of carbonaceous aerosol in two largest cities in Pearl River Delta Region, China. *Atmos. Environ.*, **41**, 2895–2903.

Forster, P., M. Blackburn, R. Glover, and K. Shine, 2000: An examination of climate sensitivity for idealised climate change experiments in an intermediate general circulation model. *Climate Dyn.*, **16**, 833–849.

Grenfell, J. L., D. T. Shindell, D. Koch, and D. Rind, 2001: Chemistry-climate interactions in the Goddard Institute for Space Studies general circulation model: 2. New insights into modeling the pre-industrial atmosphere. *J. Geophys. Res.*, **106**, D24, 33435–33451.

Griffin, R. J., D. R. Cocker, J. H. Seinfeld, and D. Dabdub, 1999a: Estimate of global atmospheric organic aerosol from oxidation of biogenic hydrocarbons. *Geophys. Res. Lett.*, **26**, 2721–2724.

Griffin, R. J., D. R. Cocker, R. C. Flagan, and J. H. Seinfeld, 1999b: Organic aerosol formation from the oxidation of biogenic hydrocarbons. *J. Geophys. Res.*, **104**, 3555–3567.

Hansen, J., A. Lacis, G. Russell, P. Stone, I. Fung, R. Ruedy, and J. Lerner, 1984: Climate sensitivity: Analysis of feedback mechanisms. Climate processes and climate sensitivity, Geophysical Monography, Hansen and Takahashi, Eds., AGU, Washington D. C., 130–163.

Hansen, J., M. Satio, and R. Ruedy, 1997: Radiative forcing and climate response. *J. Geophys. Res.*, **102**, 6831–6864.

Hansen, J., and Coauthers, 2005: Earth's energy imbalance: Confirmation and implications. *Science*, **308**, 1431–1435.

IPCC, 2001: *Climate Change 2001: The Scientific Basis*. Cambridge University Press, Cambridge, United Kingdom and New York, NY, USA, 881pp.

IPCC, 2007: *Climate Change 2007: The Physical Science Basis*. Cambridge University Press, Cambridge, United Kingdom and New York, NY, USA, 996pp.

Jacobson, M. Z., 2004: Climate response of fossil fuel and biofuel soot, accounting for soot's feedback to snow and sea ice albedo and emissivity. *J. Geophys. Res.*, **109**, D21201, doi: 10.1029/2004JD004945.

Jones, A., J. M. Haywood, and O. Boucher, 2007: Aerosol forcing, climate response and climate sensitivity in the Hadley Centre climate model. *J. Geophys. Res.*, **112**, D20211, doi: 10.1029/2007JD008688.

Joshi, M., K. Shine, M. Ponater, N. Stuber, R. Sausen, and L. Li, 2003: A comparison of climate response to different radiative forcings in three general circulation models: Toward an improved metric of climate change. *Climate Dyn.*, **20**, 843–854, doi: 10.1007/s00382-003-0305-9.

Keen, A. B., and J. M. Murphy, 1997: Influence of natural variability and the cold start problem on the simulated transient response to increasing CO_2. *Climate Dyn.*, **13**, 847–864.

Levy, H., M. D. Schwarzkopf, L. Horowitz, V. Ramaswamy, and K. L. Findell, 2008: Strong sensitivity of late 21st century climate to projected changes in short-lived air pollutants. *J. Geophys. Res.*, **113**, D06102, doi: 10.1029/2007JD009176.

Liao, H., and J. H. Seinfeld, 2005: Global impacts of gas-phase chemistry-aerosol interactions on direct radiative forcing by anthropogenic aerosols and ozone. *J. Geophys. Res.*, **110**, D18208, doi: 10.1029/2005JD005907.

Liao, H., P. J. Adams, S. H. Chung, J. H. Seinfeld, L. J. Mickley, and D. J. Jacob, 2003: Interactions between tropospheric chemistry and aerosols in a unified general circulation model. *J. Geophys. Res.*, **108**(D1), 4001, doi: 10.1029/2001JD001260.

Liao, H., J. H. Seinfeld, P. J. Adams, and L. J. Mickley, 2004: Global radiative forcing of coupled tropospheric ozone and aerosols in a unified general circulation model. *J. Geophys. Res.*, **109**, D16207, doi: 10.1029/2003JD004456.

Liao, H., W.-T. Chen, and J. H. Seinfeld, 2006: Role of climate change in global predictions of future tropospheric ozone and aerosols. *J. Geophys. Res.*, **111**, D12304, doi: 10.1029/2005JD006852.

Liepert, B. G., J. Feichter, U. Lohmann, and E. Roeckner, 2004: Can aerosols spin down the water cycle in a warmer and moister world?. *Geophys. Res. Lett.*, **31**, L06207, doi: 10.1029/2003GL019060.

Meehl, G. A., J. M. Arblaster, and W. D. Collins, 2008: Effects of black carbon Aerosols on the Indian monsoon. *J. Climate*, **21**, 2869–2882.

Menon, S., 2004: Current uncertainties in assessing aerosol effects on climate. *Annual Review of Environment Resources*, **29**, 1–30.

Menon, S., J. Hansen, L. Nazarenko, and Y. F. Luo, 2002: Climate effects of black carbon aerosols in China and India. *Science*, **297**, 2250–2253.

Mitchell, J. F. B., and T. J. Johns, 1997: On the modification of greenhouse gas warming by sulfate aerosols. *J. Climate*, **10**, 245–267.

Mickley, L. J., D. J. Jacob, B. D. Field, and D. Rind, 2004: Climate response to the increase in tropospheric ozone since preindustrial times: A comparison between ozone and equivalent CO_2 forcings. *J. Geophys. Res.*, **109**, D05106, doi: 10.1029/2003JD003653.

Nenes, A., C. Pilinis, and S. N. Pandis, 1998: Isorropia: A new thermodynamic equilibrium model for multiphase multicomponent inorganic aerosols. *Aquatic Geochemistry*, **4**, 123–152.

Ramaswamy, V., and M. M. Bowen, 1994: Effect of changes in radiatively active species upon the lower stratospheric temperatures. *J. Geophys. Res.*, **99**, D9, 18909–18921.

Ramanathan, V., and Coauthors, 2005: Atmospheric Brown Clouds: Impacts on south Asian climate and hydrological cycle. *Proceedings of National Academy of Sciences*, **102**, 5326–5333.

Rind, D., and J. Lerner, 1996: The use of on-line tracers as a diagnostic tool in general circulation model development 1. Horizontal and vertical transport in the troposphere. *J. Geophys. Res.*, **101**, 12667–12683.

Rind, D., J. Lerner, K. Shah, and R. Suozzo, 1999: Use of on-line tracers as a diagnostic tool in general circulation model development 2. Transport between the troposphere and stratosphere. *J. Geophys. Res.*, **104**, 9151–9167.

Rind, D., J. Lerner, and C. McLinden, 2001: Changes of tracer distribution in the doubled CO_2 climate. *J. Geophys. Res.*, **106**, 28061–28080.

Roeckner, E., P. Stier, J. Feichter, S. Kloster, M. Esch, and I. Fischer-Bruns, 2006: Impact of Carbonaceous Aerosol Emissions on Regional Climate Change. *Climate Dyn.*, **27**, 553–571.

Rosenfeld, D., U. Lohmann, G. B. Raga, C. D. O′Dowd, M. Kulmala, S. Fuzzi, A. Reissell, and M. O. Andreae, 2008: Flood or drought: How do aerosols affect precipitation? *Science*, **321**, 1309, doi: 10.1126/science.1160606.

Russell, G. L., J. R. Miller, and L.-C. Tsang, 1984: Seasonal ocean heat transports computed from an atmospheric model. *Dynamics of Atmospheres and Oceans*, **9**, 253–271.

Shindell, D. T., J. L. Grenfell, D. Rind, V. Grewe, and C. Price, 2001: Chemistry-climate interactions in the Goddard Institute for Space Studies general circulation model: 1. Tropospheric chemistry model description and evaluation. *J. Geophys. Res.*, **106**, D8, 8047–8075.

Shindell, D., G. Faluvegi, A. Lacis, J. Hansen, R. Ruedy, and E. Aguilar, 2006: Role of tropospheric ozone increases in 20th-century climate change. *J. Geophys. Res.*, **111**, D08302, doi: 10.1029/2005JD006348.

Shindell, D. T., H. Levy II, M. D. Schwarzkopf, L. W.

Horowitz, J.-F. Lamarque, and G. Faluvegi, 2008: Multimodel projections of climate change from short-lived emissions due to human activities. *J. Geophys. Res.*, **113**, D11109, doi: 10.1029/2007JD009152.

Sloane, C. S., 1984: Optical properties of aerosols of mixed composition. *Atmos. Environ.*, **18**, 871–878.

Sloane, C. S., 1986: Effect of composition on aerosol light scattering efficiencies. *Atmos. Environ.*, **20**, 1025–1037.

Sloane, C. S., and G. T. Wolff, 1985: Prediction of ambient light scattering using a physical model responsive to relative humidity: Validation with measurements from Detroit. *Atmos. Environ.*, **19**, 669–680.

Sloane, C. S., J. G. Watson, J. C. Chow, L. C. Pritchett, and L. W. Richards, 1991: Size-segregated fine particle measurements by chemical species and their impact on visibility impairment in Denver. *Atmos. Environ.*, **25A**, 1013–1024.

Stier, P., J. Feichter, E. Roeckner, S. Kloster, and M. Esch, 2006: The evolution of the global aerosol system in a transient climate simulation from 1860 to 2100. *Atmospheric Chemistry and Physics*, **6**, 3059–3076.

Streets, D. G., and Coauthers, 2003: An inventory of gaseous and primary aerosol emissions in Asia in the year 2000. *J. Geophys. Res.*, **108**, D21, 8809, doi: 10.1029/2002JD003093.

Streets, D. G., Q. Zhang, L. Wang, K. He, J. Hao, Y. Wu, Y. Tang, and G. R. Carmichael, 2006: Revisiting China's CO emissions after the Transport and Chemical Evolution over the Pacific (TRACE-P) mission: Synthesis of inventories, atmospheric modeling, and observations. *J. Geophys. Res.*, **111**, D14306, doi: 10.1029/2006JD007118.

Stuber, N., M. Ponater, and R. Sausen, 2001: Is the climate sensitivity to ozone perturbations enhanced by stratospheric water vapor feedback? *Geophys. Res. Lett.*, **28**, 2887–2890.

Takemura, T., T. Nozawa, S. Emori, T. Y. Nakajima, and T. Nakajima, 2005: Simulation of climate response to aerosol direct and indirect effects with aerosol transport-radiation model. *J. Geophys. Res.*, **110**, D02202, doi: 10.1029/2004JD005029.

Trenberth, K. E., 1999: Conceptual framework for changes of extremes of the hydrological cycle with climate change. *Climate Change*, **42**, 327–339.

Wang, C., 2004: A modeling study on the climate impacts of black carbon aerosols. *J. Geophys. Res.*, **109**, D03106, doi: 10.1029/2003JD004084.

Wang, C., 2007: Impact of direct radiative forcing of black carbon aerosols on tropical convective precipitation. *Geophys. Res. Lett.*, **34**, L05709, doi: 10.1029/2006GL028416.

Wild, M., A. Ohmura, H. Gilgen, and D. Rosenfeld, 2004: On the consistency of trends in radiation and temperature records and implications for the global hydrological cycle. *Geophys. Res. Lett.*, **31**, L11201, doi: 10.1029/2003GL019188.

Xu, X., W. Lin, T. Wang, P. Yan, J. Tang, Z. Meng, and Y. Wang, 2008: Long-term trend of surface ozone at a regional background station in eastern China 1991–2006: Enhanced variability. *Atmospheric Chemistry and Physics*, **8**, 2595–2607.

Yang, F., K. He, B. Ye, X. Chen, L. Cha, S. H. Cadle, T. Chan, and P. A. Mulawa, 2005: One-year record of organic and elemental carbon in fine particles in downtown Beijing and Shanghai. *Atmospheric Chemistry and Physics Discuss*, **5**, 217–241.

Yu, J., Chen, T., B. Guinot, H. Cachier, T. YU, W. Liu, and X. Wang, 2006: Characteristics of carbonaceous particles in Beijing during winter and summer 2006. *Adv. Atmos. Sci.*, **23**, 468–473, doi: 10.1007/s00376-006-0468-5.

Zhang, X.-Y., P. Zhang, Y. Zhang, X.-J. Li, and H. Qiu, 2007: The trend, seasonal cycle, and sources of tropospheric NO_2 over China during 1997–2006 based on satellite measurement. *Science in China*(*D*), **50**, 1877–1884.